CHAPTER IV
RESULTS AND DISCUSSION

4.1 Surface Activity of Produced Biosurfactants

The rhamnolipid biosurfactant was produced by bacteria *Pseudmonas aeruginosa* strain SP4, gram–negative bacteria, which excrete a mixture of biosurfactants with a glycolipids structure. The rhamnolipid biosurfactant has a unique built-in amphiphilic molecular structure consisting of hydrophilic head formed by one or two rhamnose molecules and a hydrophobic tail that contains one or two fatty acid chains. Regarding previous work (Pornsunthorntawee et al, 2007), it was found that among the fractionated components, the structure of monorhamnolipid (Rha-C_{10}-C_{10}) is the predominant component in the crude biosurfactant and the chemical structure was illustrated in Scheme 1. The rhamnolipids provide good physicochemical properties in term of surface activities, stabilities, and emulsification activities. Parra *et al.* (1989) reported that rhamnolipid surfactants can reduce the surface tension of water from 72 mN/m to values below 30 mN/m and the interfacial tension of water/oil systems from 43 mN/m to value < 1 mN/m. From surface tension measurements, the culture supernatant in this present study can reduce the surface tension of water from 72 to 28.06 %v/v as shown in Figure 4.1. Moreover, the surface tensions of the crude biosurfacatnt were also measured. Figure 4.2 shows the plot of surface tension versus initial surfactant concentration of the crude biosurfactant.

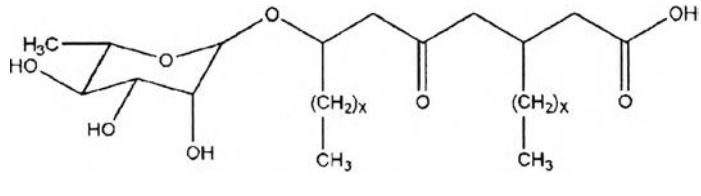

Scheme 1 Chemical structure of rhamnolipid biosurfactant.

The surface tension of the crude biosurfactant rapidly decreased as the concentration of biosurfactants increased, and a minimum surface tension of 30.4 mN/m was found at an initial biosurfactant concentration greater than 250 mg/L. From the break point of surface tension versus its log of concentration curve, the CMC of the crude biosurfactant is approximately 250 mg/L. The obtained values of the CMC of the crude biosurfactant and the minimum surface tension are consistent with the previously report (Pornsunthorntawee et al, 2007).

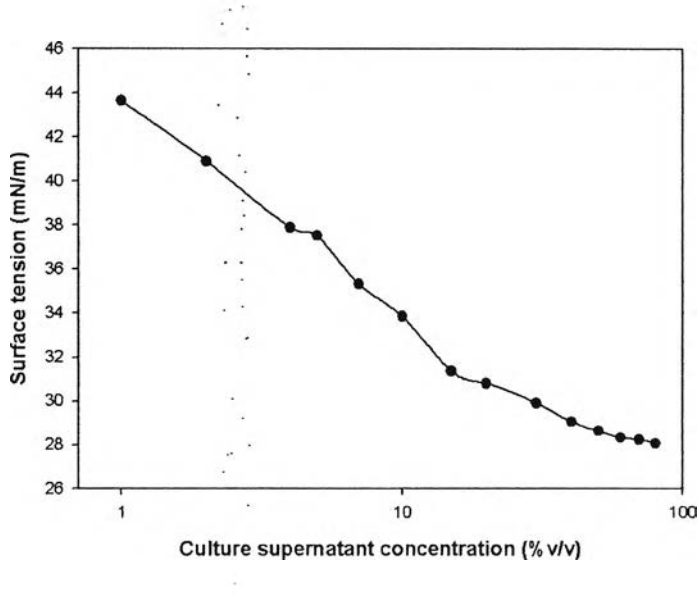

Figure 4.1 Surface tension versus the culture supernatant concentration produced by *Pseudmonas aeruginosa* strain PS4.

Moreover, a biosurfactant also exhibit stability and emulsification properties as well. Benincasa *et al.* (2004) reported that the biosurfactant produced by *Pseudomonas aeruginosa* LBI could form stable emulsions with *i*-propyl palmitate, castor oil, almond oil, crude oil, kerosene, and benzene for 21 days. Wei *et al.* (2005) revealed the biosurfactant also achieved a maximum emulsion index of 70% and 78%, for diesel and kerosene, respectively, at a low concentration of about 300 mg/L. As a result, amphiphilic biosurfactant molecule can form emulsion with various kinds of oils because it is active to form micelles and stabilize the dispersion in the reaction medium. Interestingly, the micelle of biosurfactant can trap some

hydrophobic substances suggesting the possibility to serve as the template for the accumulation of hydrophobic-like aniline molecule and subsequent polymerization.

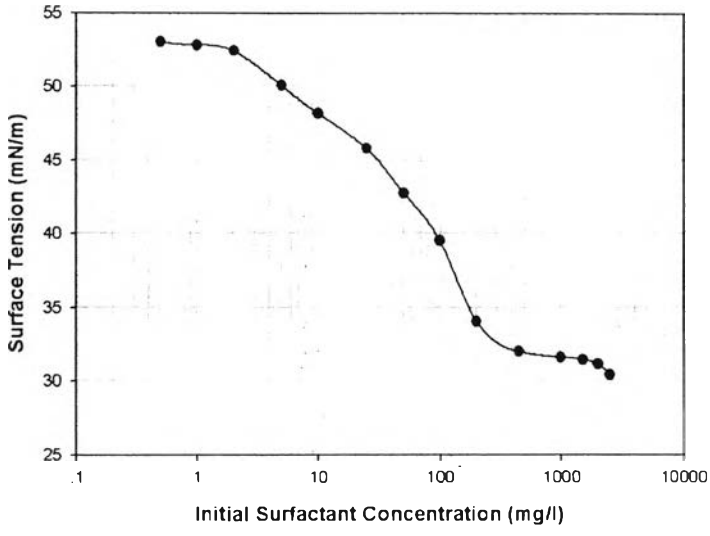

Figure 4.2 Surface tension versus concentration of crude biosurfactant produced by *Pseudmonas aeruginosa* strain SP4.

The addition of an aniline monomer, the studied monomer in this work, into the aqueous solution of biosurfactant under magnetically stirring could produce a milky emulsion. In order to understand the existance of morphology as well as the formation mechanism of the obtained product, we did emulsification testing between aniline monomer (ANI) and biosurfactant solution by varying the ANI:Biosurfactant weight ratio at constant biosurfactant concentration equal to 1800 mg/L as shown in Figure 4.3.

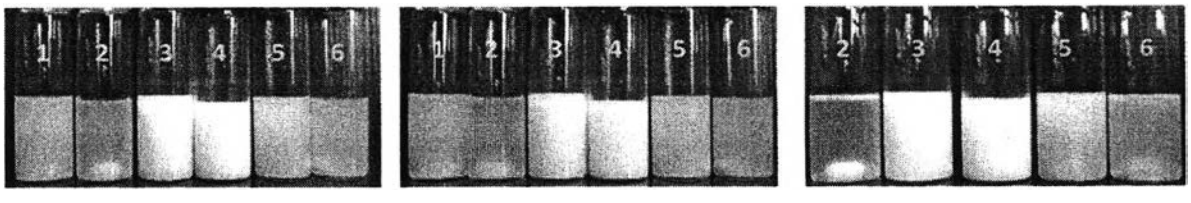

Figure 4.3 ANI+biosurfactant solution complex after left (a) 24 hr; (b) 48 hr; (c) 72 hr. 1=ANI monomer dissolved in distillation water; 2=1800 mg/l biosurfactant

dissolved in distillation water; ANI+biosurfactant complex at ANI:Biosurfactant weight ratio of 3=28.3:1, 4=22.7:1, 5=19.3:1, 6=11.3:1.

From emulsification testing, it indicated that the biosurfactant was able to emulsify ANI monomer at ANI:Biosurfactant weight ratio equal to 28.3:1 and 22.7:1 for more than 72 hours by forming a milky solution. Interestingly, at the weight ratio of 22.7:1, we found that it can form the longest stable milky emulsion for more than 1 week under a static condition. On the other hand, at ANI:Biosurfactant weight ratio of 19.3:1, the thick milky emulsion transformed into a pale emulsion. Additionally, at ANI:Biosurfactant weight ratio equal to 11.3:1, they cannot form milky solution and found to undergo phase separation after left overnight. It suggested that, at concentration of 1800 mg/L, the rhamnolipid biosurfactant can emulsify the ANI monomer at ANI:Biosurfactant weight ratio equal to 28.3:1, 22.7:1, and 19.3:1 and these concentration were utilized as a template to synthesize the polyaniline (PANI) nanoparticles.

4.2 Synthesis of Polyaniline Nanoparticles by Using the Biosurfactant as a Template

Highly order PANI was synthesized by an oxidative polymerization of aniline monomer under the acidic condition. Unfortunately, the emulsify property of biosurfactant template could not be toterance in the strong acid condition. Therefore, in this experiment we tried to find the suitable acid concentration for using as the condition for polymerization of aniline.

4.2.1 Effect of Acid Concentration

The effect of acid concentration was investigated in order to study the minimum acid concentration in the reaction medium that could obtain PANI existed in the emeraldine salt form (PANI ES), the conducting state of PANI, and study the effect of acid concentration on the morphology of the synthesized PANI. It was found at 0.01 M HCl, the polymerization reaction was incomplete, and the solution exhibited in the color of straw as shown in Figure 4.4-c. However, with increase of HCl concentration the color turn to turquoise-black color. This implies the

importance of the acid concentration on the polymerization reaction. Figure 4.4 show the SEM images of PANI synthesized with different acid concentration as well as 0.01M, 0.1M, 0.5M, and 1.0M HCl concentration at 6 h polymerization time. The images revealed that the acid concentration had a significant effect on morphology of the resulting PANI. Interestingly, it was observed that the fibrillar structure of PANI, with the average diameter of 121 nm ± 18 nm, was obtained at the concentration of 0.1M HCl. On the other hand, at acid concentration of 0.01 M, 0.5 M, and 1.0M, the coral-like structure were observed and the morphology similar to the morphology of PANI synthesized by conventional approach. Moreover, the remaining biosurfactant was observed on the synthesized PANI product when using 0.01M HCl acid concentration. Figure 4.4-d also illustrated that PANI exist in the form of nanofibers structure and exhibit the well dispersion in the medium for more than 1 day. In contrast, existence of the obtained PANI in the aggregation form rapidly precipitating from the medium.

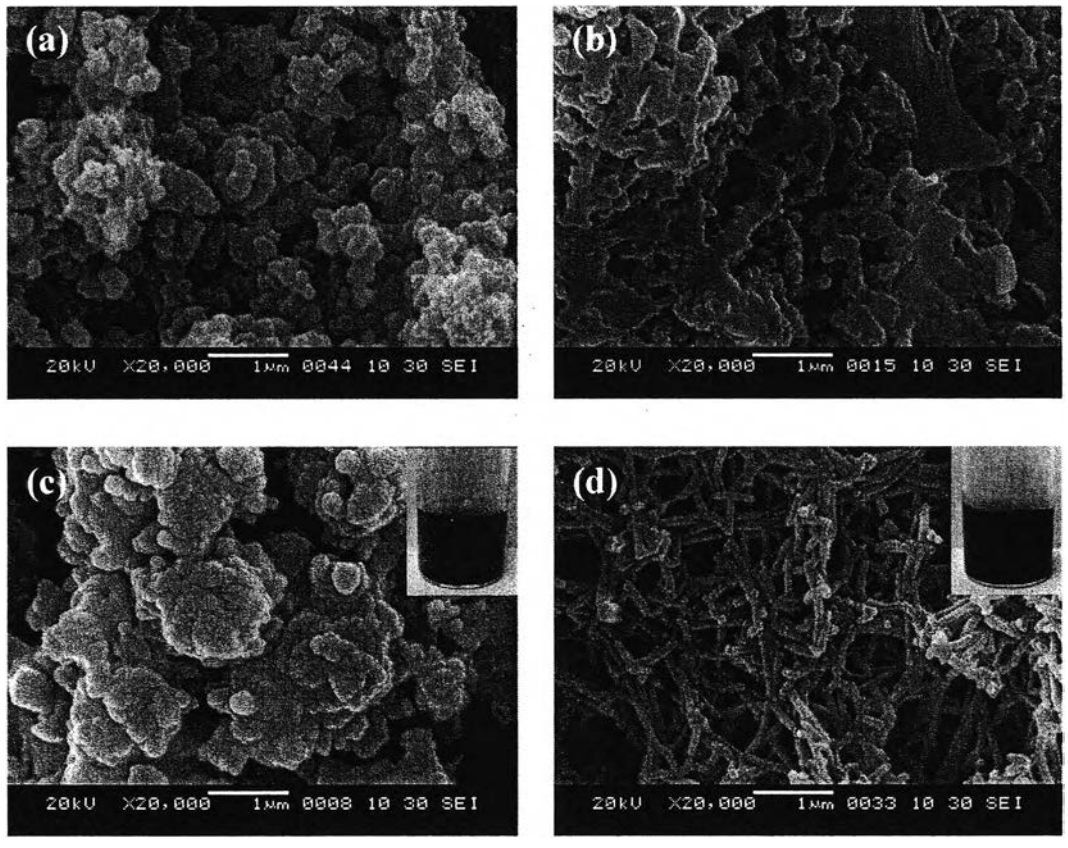

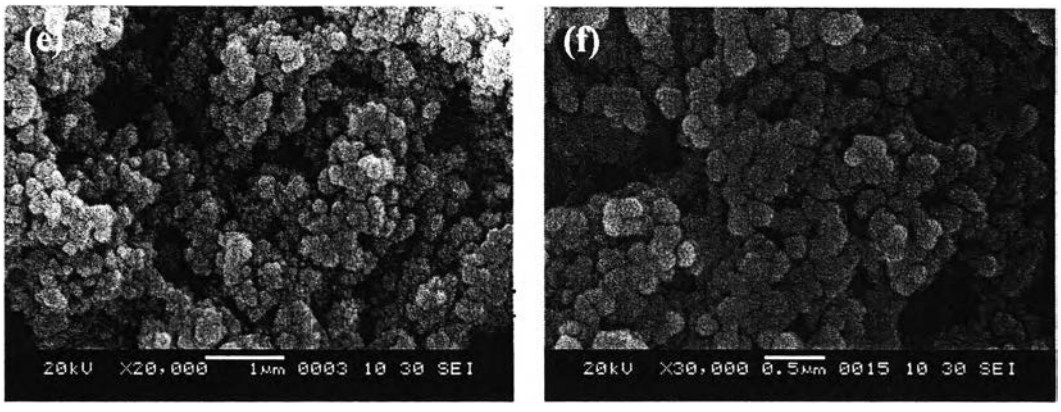

Figure 4.4 SEM images of a) conventional PANI; b) before remove template of PANI 0.1M HCl; and PANI polymerized in the presence of various acid concentration at the ANI:Biosurfactant weight ratio equal to 22.7:1 after dialysis with mixture solution of distillation water and ethanol; c) 0.01M; d) 0.1M; e) 0.5M; and f) 1.0M HCl.

4.2.2 Effect of ANI:Biosurfactant Weight Ratio

Scanning electron microscopy (SEM) and Transmittion electron microscope (TEM) was used to investigate the morphology of the synthesized PANI obtained by using 0.1M HCl acid concentration at different ANI:Biosurfactant weight ratio as shown in Figure 4.5. From SEM, the irregularly-shaped PANI aggregates were observed in the PANI synthesized by the conventional method, as shown in Figure 4.5-a. In contrast, on the adding of the biosurfactant into the polymerization media, the fibrillar structure of PANI was formed. It was found that the average diameter (based on a sample of n=50 particles) of the obtained PANI nanofiber gradaully decreased, at fixed biosurfactant content (1800 mg/L), from 151.6 ± 13 nm to 121.0 ± 18 nm and 121.2 ± 12 nm when the ANI:Biosurfactant ratio was decreased from 28.3:1 to 22.7:1 and 19.3:1, respectively (Figure 4.5 b-d). However, at ANI:Biosurfactant weight ratio of 11.3:1, the fibrillar structure was not observed (Figure 4.5-e).

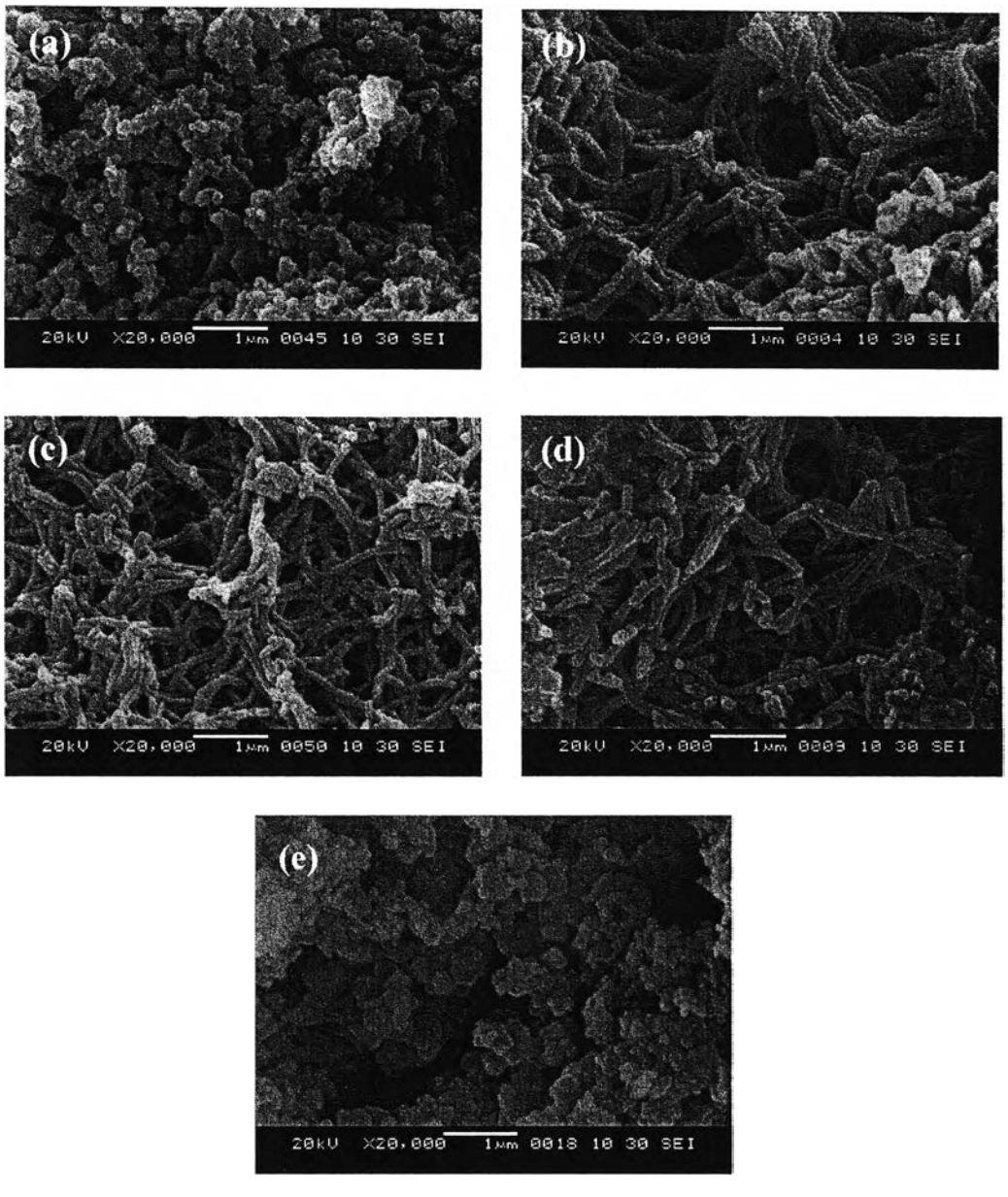

Figure 4.5 SEM images of a) conventional PANI; and PANI polymerized in the presence of different ANI:Biosurfactant weight ratio at constant 1800 mg/L biosurfactant after dialysis with mixure solution of distillation water and ethanol: b) 28.3:1; c) 22.7:1; d) 19.3:1; and e) 11.3:1.

Since the SEM technique is inadequate to see the internal features of nanofibers structure, thus the samples were subjected to TEM analysis. TEM image of PANI synthesized at ANI:Biosurfactant weight ratio of 28.3 exhibited dense

nanorod structures as shown in Figure 4.6-a. Interestingly, the TEM image of PANI synthesized at weight ratio of 22.7:1 consists of a mixture of nanotubes and nanorods showed in Figure 4.6-b. However, the TEM image of the resulting PANI before remove biosurfactant template was also investigated as shown in Figure 4.6-c.

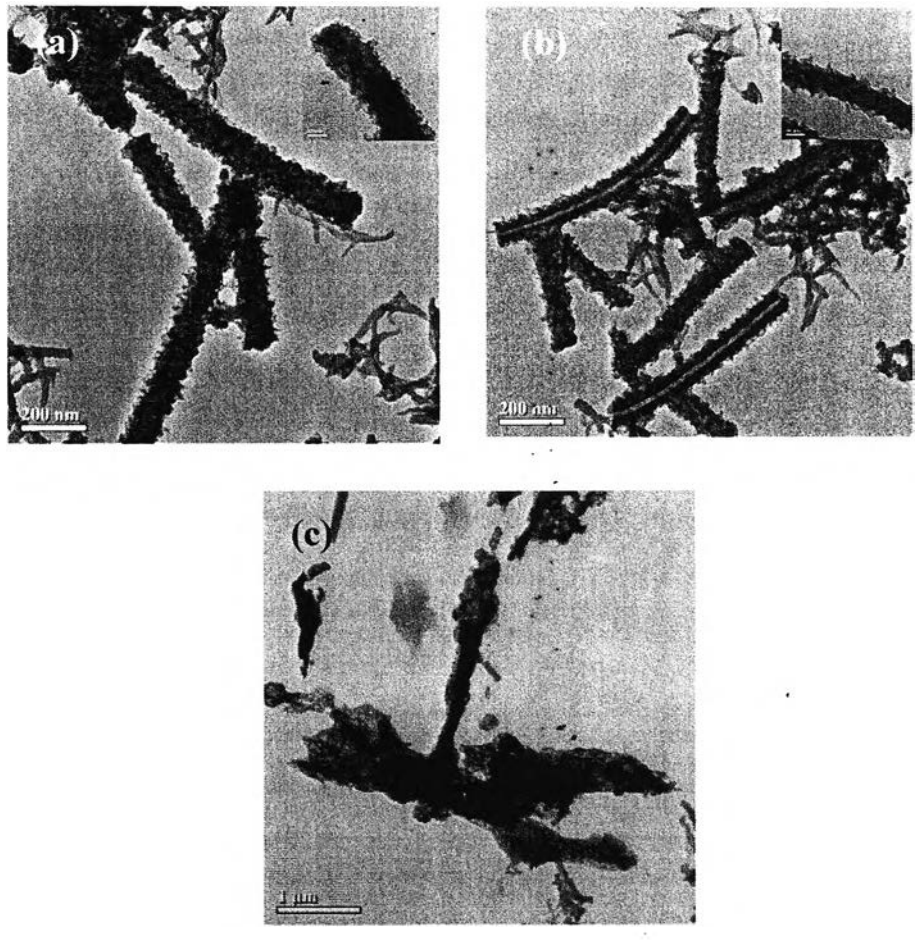

Figure 4.6 Transmission Electron Microscopy (TEM) images of PANI polymerized in the presence of different ANI:Biosurfactant weight ratio at constant 1800 mg/L biosurfactant after dialysis with mixture solution of distillation water and ethanol: a) 28.3:1; b) 22.7:1 and c) PANI before remove biosurfactant template.

The formation of nanostructure was explained based on the nucleation and growth theories. Li et al. (2008) reported that the formation of PANI is initiated by some nuclei that can be formed homogeneously in the parent phase or they can be heterogeneously grown on other species such as preformed particles or the reactor

surface. In order to trace the formation mechanism of PANI nanofiber synthesized in the present of biosurfactant as a template, the dynamic light scaterring (DLS) and transmission electron microscopy (TEM) was used to study the aggregation behavior of the biosurfactant in condition of distillation water, aniline monomer, and acidic solution. TEM micrograph of 1800 mg/L biosurfactant concentration show the vesicular structure and the DLS show a size distribution with the hydrodynamic diameter of 126 nm which are classified as a medium vesicular structure as shown in Figure 4.7-a . From previous work, Champion et al. (1994) classified the size of vesicle as the aggregates with the size smaller than 50 nm are responsible for small vesicle. On the other hand, the aggregates with the sizes in the range of 50 to 250 nm are classified as a medium vesicular structure and the size of aggregate larger than 250 nm are considered to be a large vesicular structure. Furthermore, after adding aniline into the biosurfactant solution, a thick milky emulsion was formed and the aggregation of aniline in biosurfactant solution was shown in Figure 4.7-b. In addition the DLS indicated that the vesicular become larger 67% and exist in the hydrodynamic diameter of 211 nm. Additionally, when 0.1 M HCl was added into the mixture solution of aniline and biosurfactant, the profile of the DLS measurement show a distribution with the hydrodynamic diameter of 241 nm. The increasing in size of the vesicular structure after the addition of aniline monomer and 0.1M HCl into the biosurfactant solution due to the formation of the hydrogen bonding and electrostatic interaction between amino group of aniline and biosurfactant molecule. However, in order to confirm the existence of biosurfactant during the polymerization proceeding the ammonium persulfate (APS), oxidizing agent, was added into the 1800 mg/L biosurfactant solution. After adding APS to the biosurfactant solution, the solution become pale and stable for more than 24 h at room temperature and the DLS show a size distribution with the average size of 689 nm as shown in Figure 4.7-e.

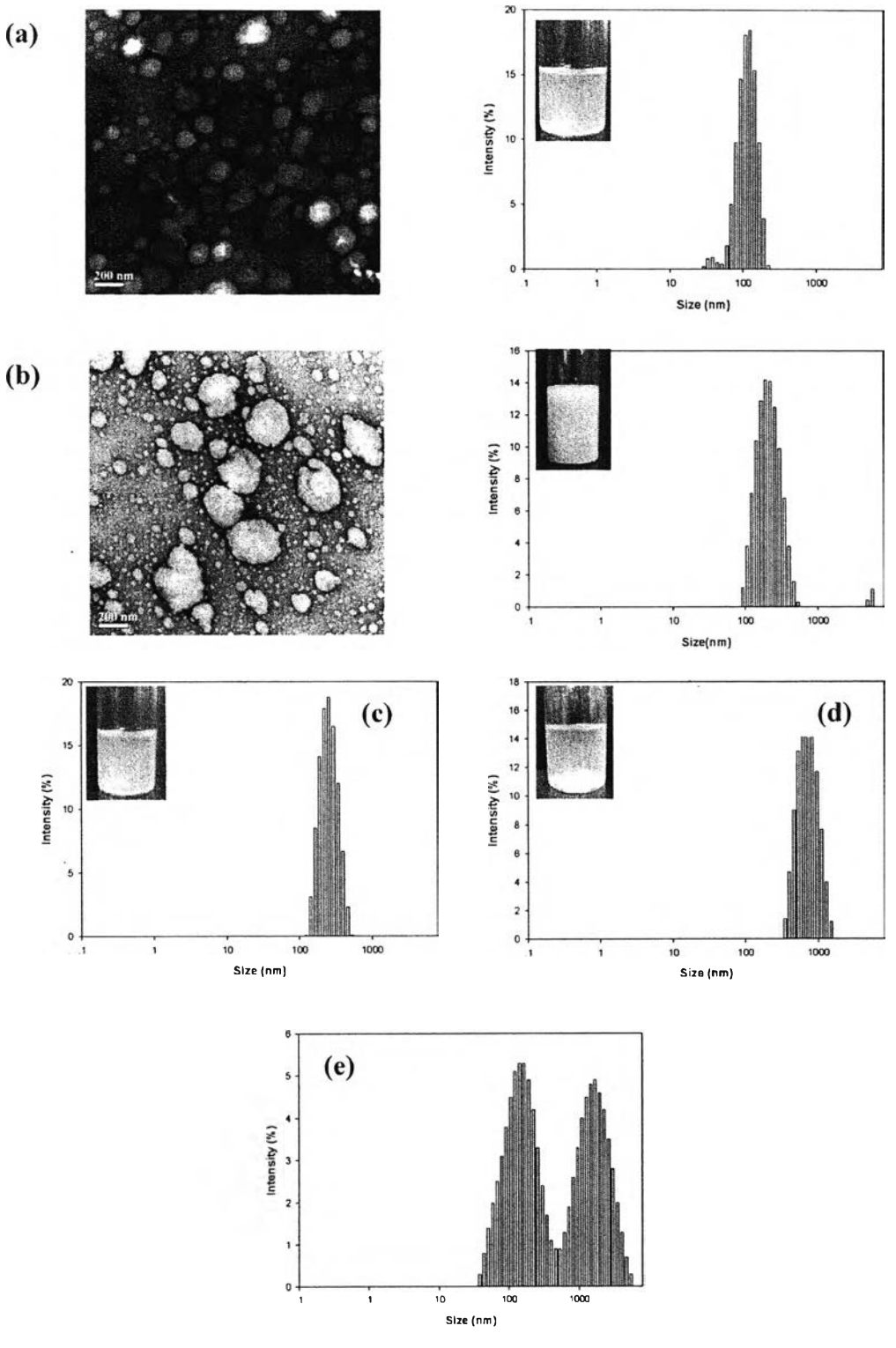

Figure 4.7 Transmission Electron Microscopy (TEM) and Dynamic light scattering measurement (DLS) of a) 1,800 mg/L biosurfactant in distillation water; b) biosurfactant solution + aniline; c) biosurfactant solution + aniline + 0.1M HCl; d)

biosurfactant solution + APS complexs and e) 3,600 mg/L biosurfactant in distillation water.

For the propose formation mechanism of the formation of PANI nanostructure synthesized in the present of the biosurfactant as a template was depicted in Scheme 2. Firstly, the vesicular structure was form after the biosurfactant was dissolved in the distillation water. And then, after the addition of aniline monomer into the biosurfactant solution, the thick milky emulsion was formed and aniline monomer prefer to penetrate into the hydrophobic part of the vesicular structure due to hydrophobic characteristic of aniline thus causing the vesicular structure became larger. After acid solution was added into the milky solution, the low polarity amino groups ($-NH_2$) of aniline are converted to higher polarity protonated forms ($-NH_3^+$). On the other hand, higher polarity biosurfactant molecules ($-COO^-$) protonated to lower polarity acid form (-COOH) resulting in hydrogen bond form occurred as shown in Scheme 3. However, the complexation can form via biosurfactant molecule existed in the form of $R–COO^-$ with anilinium cation ($-NH_3^+$). Kuramoto et al (1994) reported that sodium dodecylsulfate (SDS) anion form complexation with anilinium cation through electrostactic interaction as shown in Scheme 4. In addition, Han et al. (2008) also reported dodecylbenzenesulfonic acid (DBSA) molecules completely dissolved in hexane and create anilinium-DBSA complex because DBSA is both an anionic surfactant and an acidic catalyst.

Moreover, hydrophobic interaction between benzenoid amine and biosurfactant hydrophobic part may be occurred due to the reaction medium is within the aqueous solution. Since the reaction is within the aqueous solution the hydrophilic part will be directed outwards to the reaction medium and act as the nucleation site at the interface of the vesicle to form the vesicle A, as shown in Scheme 1. At the addition of the oxidant (APS), the polymerization takes place initially on the surface of the vesicles. Through the polymerization proceeding, the vesicle became elongate through aggregation and elongation process depending on the local condition. Finally, PANI nanotubes were obtained.

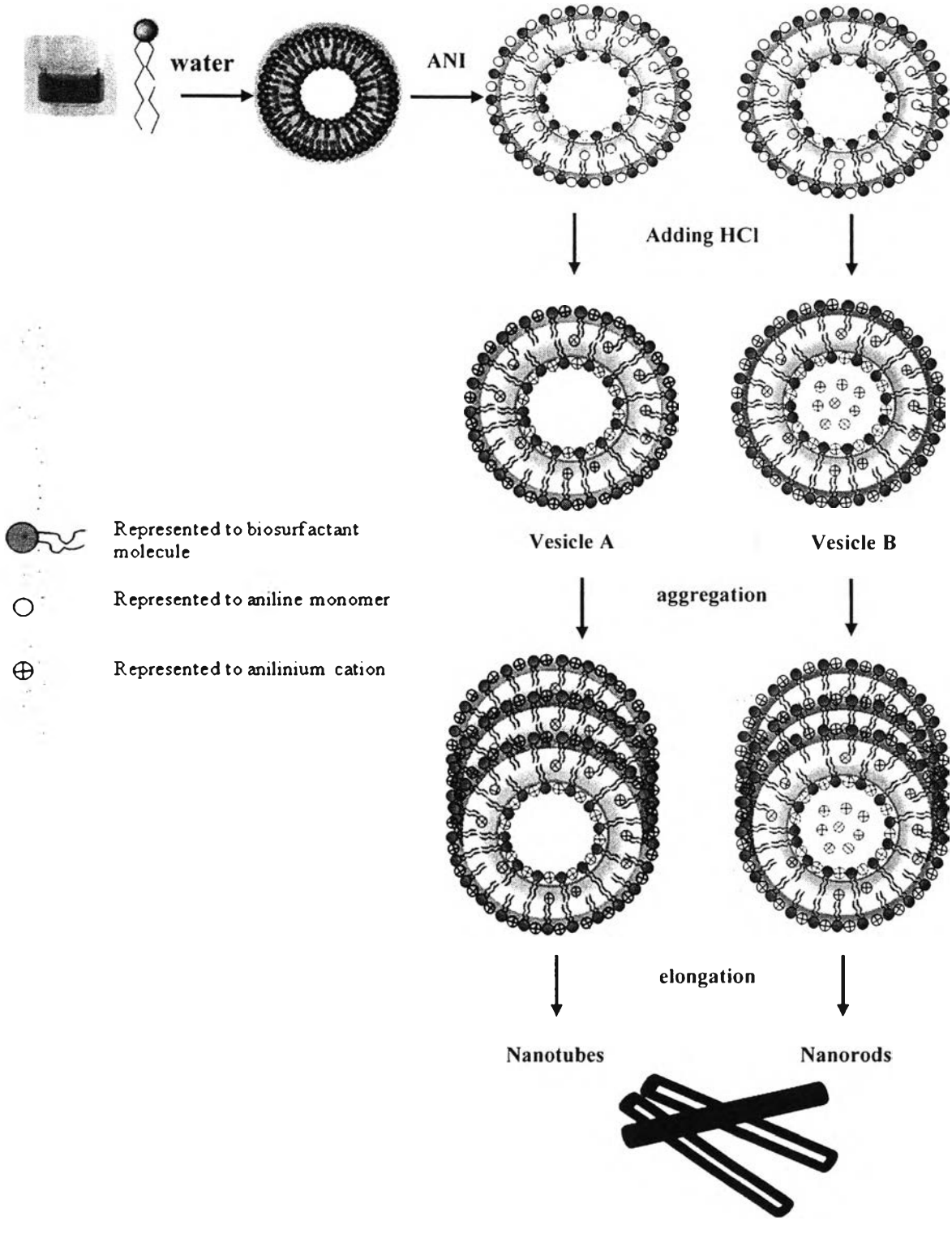

Scheme 2 Proposed formation mechanism for PANI nanostructured using a biosurfactant as a template.

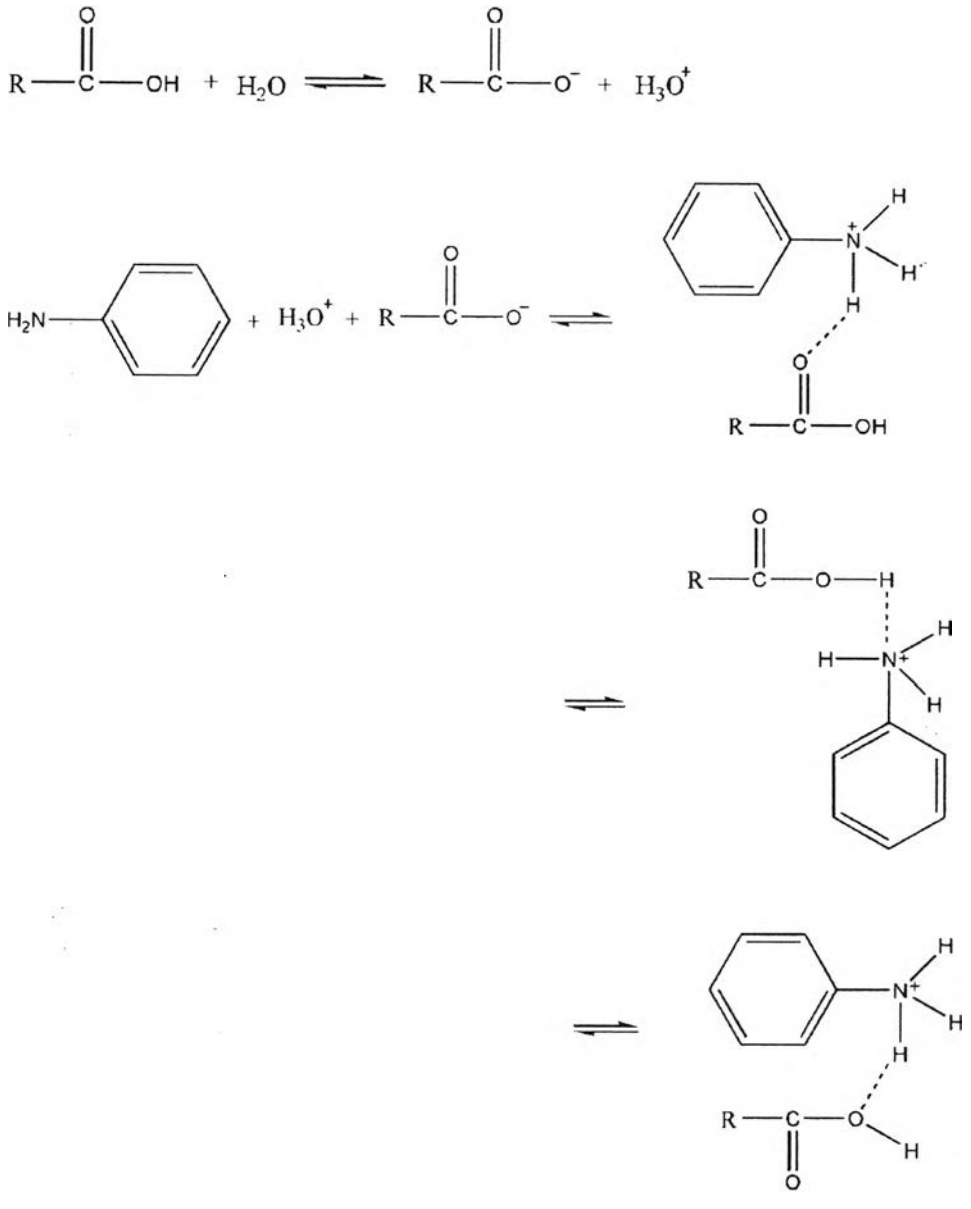

Scheme 3 H-bond formed between amine group of aniline and carboxylic group of biosurfactant.

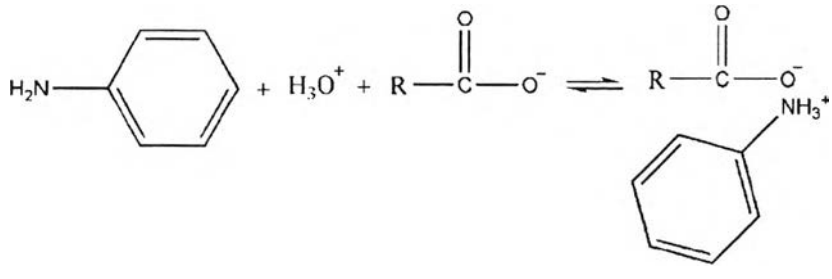

Scheme 4 Electrostatic interaction between amine group of aniline and carboxylate group of biosurfactant.

However, when increase the ANI:Biosurfactant weight ratio some anilinium cation can migrate into the hydrophilic core of the vesicular structure and the vesicle B was formed. After adding oxidizing agent, the aggregation and elongation precess occurred and finally PANI nanorods were obtained. The TEM micrograph can confirm that PANI synthesized at the ANI:Biosurfactant weight ratio of 28.3:1 illustrated the dense nanorod structure. Moreover, In our work, it is apparent that the occurrences of elongation procedure adjudicate from the morphology of the resulting PANI before remove template as shown in Figure 4.6-c . Yang et al. (2005), Anikumar et al (2008) and Zhang et al. (2002) also reported that the micelles were regarded as the templates to further produce PANI nanofibers and the fiber structures are assembled by the micelles through aggregation and elongation depending on the local conditions.

4.2.3 Effect of Reaction Time on Morphology

To gain further insight into the mechanism of formation of PANI nanofiber by oxidative polymerization, a small quantity of PANI product was collected from the polymerization media at time of 4, 6, and 8 h after addition of APS, the oxidizing agent, for SEM study. The results of which are shown in Figure 4.8. The nanofibers structure with the average diameter of 116.1 nm ± 11 nm was formed at the early stage of polymerization time (4h). However, for a longer reaction time of 6 and 8 h, PANI still forms nanofibers morphology with the average diameter of 121.0 nm ± 18 nm and 177.5 nm ± 53 nm, respectively. These appeared results due to the interval time for anilinium cation attack to nucleation site are increased as

the polymerization time increased causing the polymer chain are grown further along within the biosurfactant template. As illustrated in Figure 4.8, the nanofibers diameter increase with polymerization time increased.

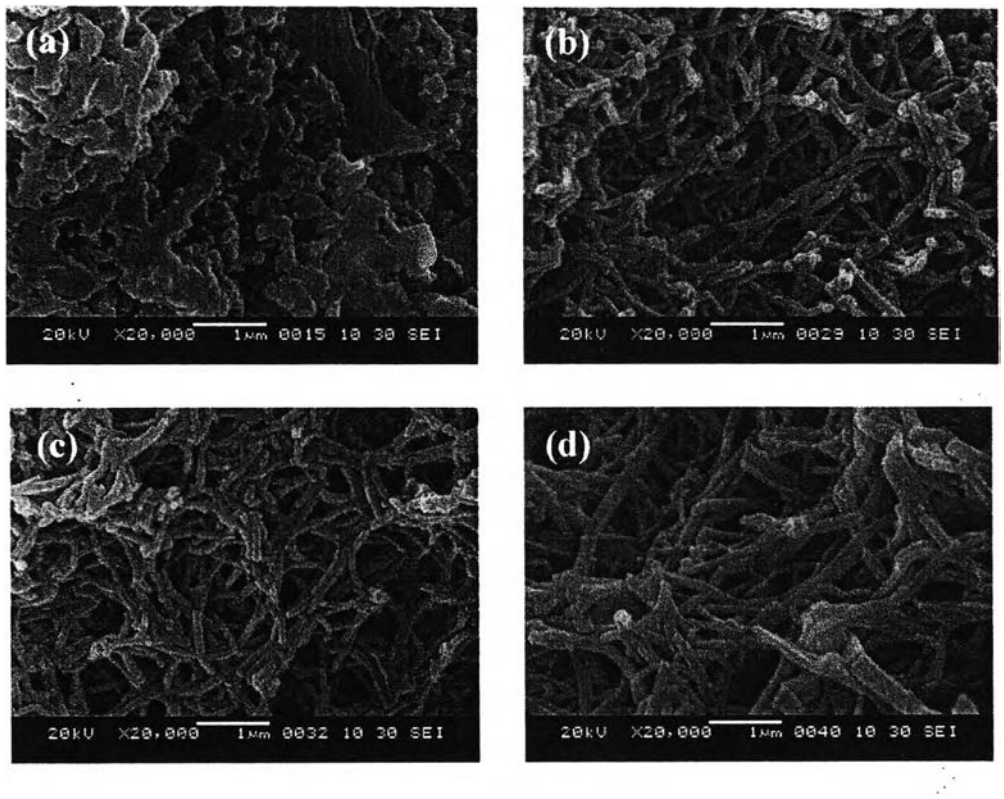

Figure 4.8 SEM images of a) PANI before remove biosurfactant template; and PANI polymerized at the different reaction time in the presence of ANI:Biosurfactant weight ratio equal to 22.7:1 at 1800 mg/L biosurfactant after dialysis with mixed distillation water and ethanol; b) 4 h; c) 6 h; d) 8 h.

4.2.4 Effect of Biosurfactant Concentration on Morphology

In order to study the effect of biosurfactant concentration on the formation of PANI, the biosurfactant concentration was increased from 1800 mg/L to 3600 mg/L and was calculated to the weight ratio of ANI:Biosurfactant equal to 14.2:1, 11.4:1, and 9.6:1. The SEM images of the obtained PANI nanofibers at such weight ratio are showed in Figure 4.9.

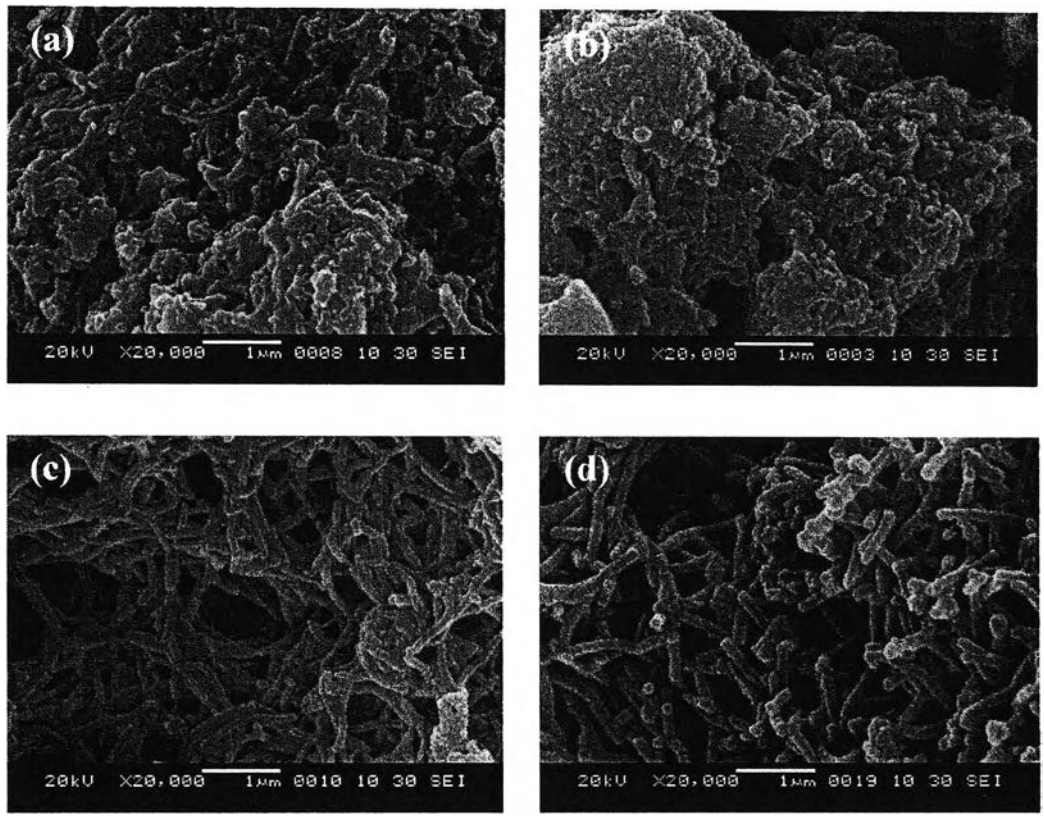

Figure 4.9 SEM images of a) PANI before remove biosurfactant template; and PANI polymerized in the presence of different ANI:Biosurfactant weight ratio at 3600 mg/L biosurfactant after dialysis with mixture solution of distillation water and ethanol: b) 14.2:1; c) 11.4:1; and d) 9.6:1.

There was different among these samples on their morphology. It was found that the average diameter (based on a sample of n=50 particles) of PANI nanofiber decreased, at fixed rhamnolipid biosurfactant content (3600 mg/l), from 144.2 nm ± 22.0 nm to 131.5 nm ± 12.3 nm when weight ratio was decreased from 11.3:1 to 9.6:1 , respectively, as shown in Figure 4.9c-d. In contrast, the coral-like structure was found at weight ratio of 14.2:1 present in the reaction medium (Figure 4.5-b). Li et al. (2008) reported that heterogeneous nucleation predominates at the later stage, and new polyaniline molecules prefer to grow on previously formed particles, resulting in the formation of coral-like particles. When compare the average diameter of PANI synthesized using 1800 mg/L and 3600 mg/L

biosurfactant concentration. It was found that the average diameter of PANI synthesized with 3600 mg/L biosurfactant were larger than PANI synthesized with 1800 mg/L biosurfactant. This result might be due to size of the resulting PANI depends on the size of biosurfactant template. Therefore, The DLS experiment was used to verify the aggregation size for both concentration of biosurfactant template. According to the DLS experiment, a distribution with the maximum aggregation size of 126 nm was investigated in the biosurfactant concentration of 1800 mg/l as shown in Figure 4.7-a. On the other hand, a bimodal distribution with maxima centered of 162 nm and 1.82 μm was observed in the biosurfactant concentration of 3600 mg/l as shown in Figure4.7-e. The DLS experiment comfirm that using higher biosurfactant concentration result in larger aggregation structure was formed and causing obtained larger diameter of the resulting PANI, while smaller in diameter of the resulting PANI was obtained instance of lower biosurfactant concentration was used as a template. Wei et al. (2001) reported that the diameter of the obtained nanofibers was controlled by [NSA]/[ANI] ratio, β-naphthalene sulfonic acid (β-NSA) acted as a dopant and template, causing the outer diameter of the resulting PANI was decreased from 650 nm to 76 nm when the [NSA]/[ANI] ratio decreased from 2 to 0.25. Zhang et al. (2002) also indicated that when using hexadecyltrimetryammonium bromide (HTAB) as a surfactant, the average diameter of PANI nanostructures varied from 180 nm to 200 nm with the concentration of HTAB changing from 0.008 to 0.016 M. This appear result indicated that the size of the obtained nanostructure depend on the concentration of the template.

4.3 Yields (%) of the Synthesized Polyaniline

4.3.1 Effect of ANI:Biosurfactant Weight Ratio

The yields (%) of the synthesized PANI were calculated, as shown in Figure 4.10, after the resulting product was dried under reduced pressure for 3 days. In conventional approach, it was found that yields (%) decreased with increase in an amount of ANI monomer adding in the reaction medium. Furthermore, in the template approach, using biosurfactant concentration of 1800 mg/L as a template, the result also show the same trend which yields (%) decrease with increasing in the

ANI:Biosurfactant weight ratio. Regarding yields (%) of the obtained product, no significant difference in percentage of yields was observed between conventional approach and biosurfactant template approach. This appear result indicated adding biosurfactant template in the reaction medium does not effect to the resulting product.

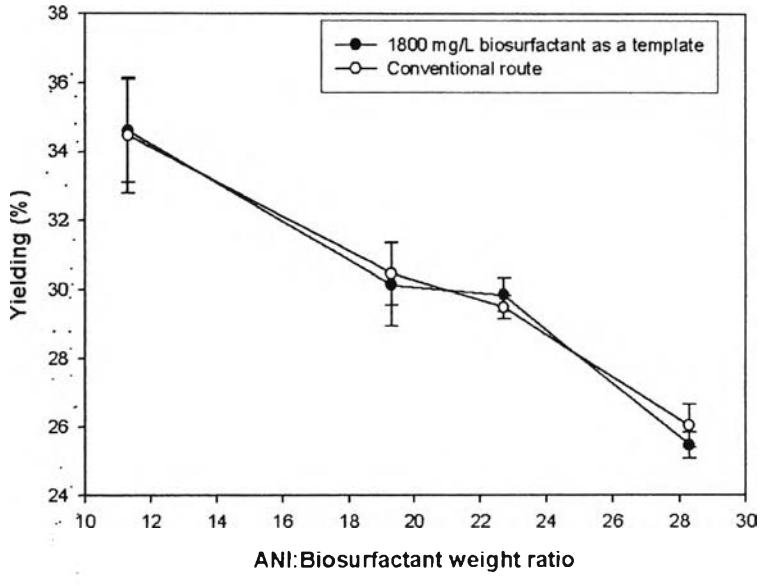

Figure 4.10 Yields (%) of the synthesized PANI at different ANI:Biosurfactant weight ratio.

4.3.2 Effect of Polymerization Time

The yields (%) of PANI as function of polymerization time also was calculated and showed in table 4.1. It was found that the percentage of yields increase with increasing the polymerization time. These appear results due to increasing the polymerization time seem like increasing the time for anilinium ion attack at nucleation site to promote the para-substitution or head-to-tail coupling of the anilinium ion radical. Therefore, yields (%) increase as function of polymerization time. In addition, Jeevananda et al. (2008) also reported that yields (%) of PANI increased from 60% to 85% as the polymerization time increased from 2 to 24 h.

Table 4.1 Yield (%) data of PANI nanomaterial as function of polymerization time

ANI:Biosurfactant weight ratio	Polymerization time (hr)	Yield (%)
22.7 : 1	4	25.78±1.02
22.7 : 1	6	29.86±0.49
22.7 : 1	8	36.55±2.70

4.3.3 Effect of Biosurfactant Concentration

Moreover, the effect of biosurfactant concentrations on percent of yields was studied as well, as shown in table 4.2. The biosurfactant concentration was increased from 1800 mg/L to 3600 mg/L and was calculated to ANI:Biosurfactant weight ratio of 14.2, 11.4, 9.6, and 5.6. The result indicated increase in weight ratio causing percent of yields decreased and no significant difference of yields were investigated between both of template approach (1800 mg/L and 3600 mg/L biosurfactant concentration as a template) as well as conventional approach. These results indicated that increasing the biosurfactant concentration does not affect to yields (%) of the resulting product.

Table 4.2 Yield (%) data of PANI nanomaterial as increase biosurfactant concentration to 3600 mg/l

ANI:Biosurfactant weight ratio	Polymerization time (hr)	Yield (%)
14.2:1	6	23.89±0.39
11.4:1	6	29.21±0.75
9.6:1	6	28.99±0.33
5.6:1	6	33.30±0.98

4.4 Characterization of the Synthesized Polyaniline

4.4.1 FTIR Spectroscopy

The FTIR characterization technique was use to identify the chemical structure of rhamnolipid biosurfactant and the resulting PANI synthesized by using various acid concentrations as shown in Figure 4.11.

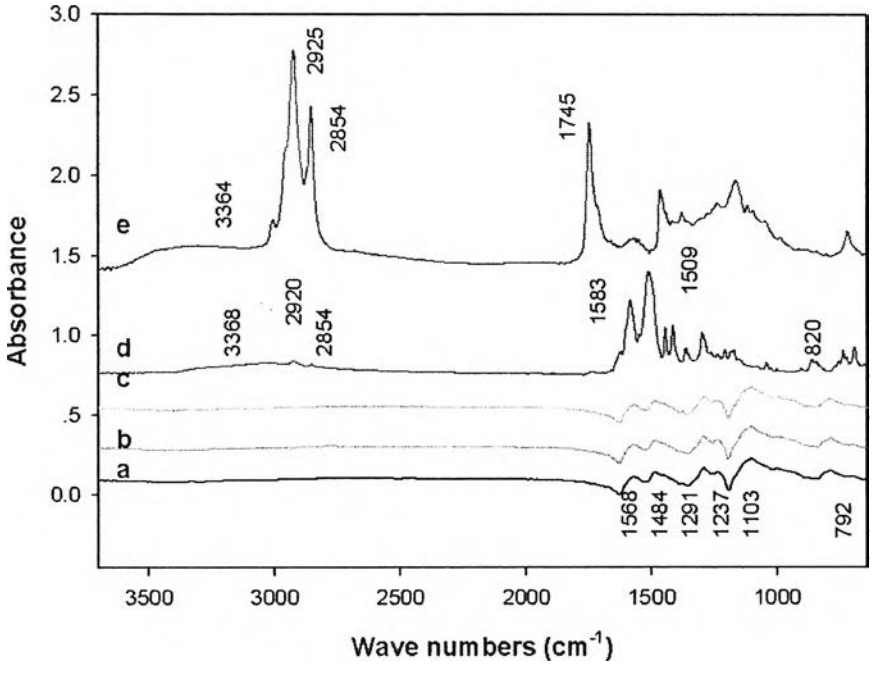

Figure 4.11 FTIR spectra of PANI synthesized using different HCl acid concentration a) 1.0M; b) 0.5M; c) 0.1M; and d) 0.01M; e) crude biosurfactant.

Figure 4.11-e shown the FTIR spectra of biosurfactant. The characteristic peaks obsearved at 3364, 2925, 2854, 1745, and 1300–1100 cm^{-1}were attributed to O–H stretching vibrations of hydroxyl groups, C–H stretching vibrations of the hydrocarbon chain, C–H stretching vibrations of hydrocarbon chain, C=O stretching vibrations of the carbonyl groups, and bonds formed between carbon atoms and hydroxyl groups in the chemical structures of the rhamnose rings, respectively.

On the contrary, the FTIR spectra of PANI synthesized using 0.1M, 0.5M, and 1.0M HCl acid concentration (Figure.4.11a-c), absorption peaks were observed at 1568, 1484, 1291, 1103 and 792 cm^{-1} assigned to C=C stretching of the quinoid ring, C=C stretching of the benzenoid ring, C-N stretching, N=Q=N stretching (Q representing the quinoid ring), and C-H out-of- plane vibration of 1,4-disubstituted benzene ring, respectively. These absorption peaks are characteristic of the emeraldine salt or doped state of PANI (PANI ES). The FTIR spectra of PANI synthesized using 0.01M HCl acid also investigated as shown in Figure 4.11-d. It was found that the spectra peaks shift to higher wave number located at 1583, 1509, 1299, and 820 cm^{-1}, respectively, these peaks are characteristic peak of undope state of PANI (PANI EB). Additionally, these adsorption band also appear peaks located at 3368, 2920, 2854, 1745; and 1300–1100 cm^{-1} which identical to those of rhamnolipids structure. This appear result was consistent with the SEM image (as shown in Figure4.4-c) indicating an incomplete removal of biosurfactant template out of the structure of the synthesized PANI.

Furthermore, Figure 4.12a-d demonstrated the chemical structure of PANI nanofiber using different ANI:Biosurfactant weight ratio. The absorbtion peak showed characteristic peak of emeraldine salt (PANI ES) and no significant difference in characteristic peaks of such PANI samples although the weight ratios are different. Moreover, the absorption peak of the resulting PANI between the template route and conventional route are the same as well. These appear results indicated that the different in ANI:Biosurfactant weight ratio does not affect to the chemical structure of the resulting PANI. On the other hand, shifts of these peaks to higher wave numbers at 1584, 1501, 1299, and 820 cm^{-1}, respectively (Figure 4.12-b), were revealed in the PANI powder after immersed in 0.4M NaOH for 3.5 hours. This indicates the emeraldine base or undoped state of PANI (PANI EB) due to deprotonation reaction occured.

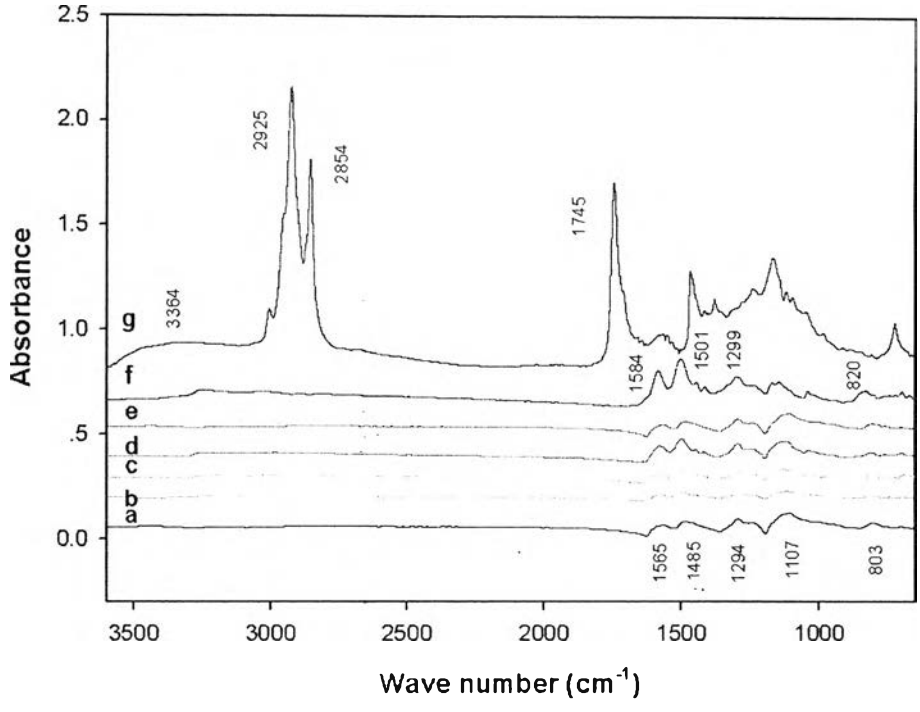

Figure 4.12 FTIR spectra of PANI synthesized at different ANI:Biosurfactant weight ratio, (a) 11.3:1; (b) 19.3:1; (c) 22.7:1; (d) 28.3:1; (e) conventional PANI; (f) undoped state of PANI (PANI EB); (g) crude biosurfactant.

The FTIR spectra of PANI synthesized at higher biosurfactant concentration (3600 mg/L) also illustrated the similar pattern with PANI synthesized by biosurfactant concentration of 1800 mg/L approach as well as conventional approach, as shown in Figure 4.13. Moreover, after dialysis the resulting product with mixture solution of ethanol and distillation water, it was found that the spectra peak of PANI products did not appear the characteristic peak of biosurfactant, therefore, it was confirmed that the obtained PANI complete removal of biosurfactant template.

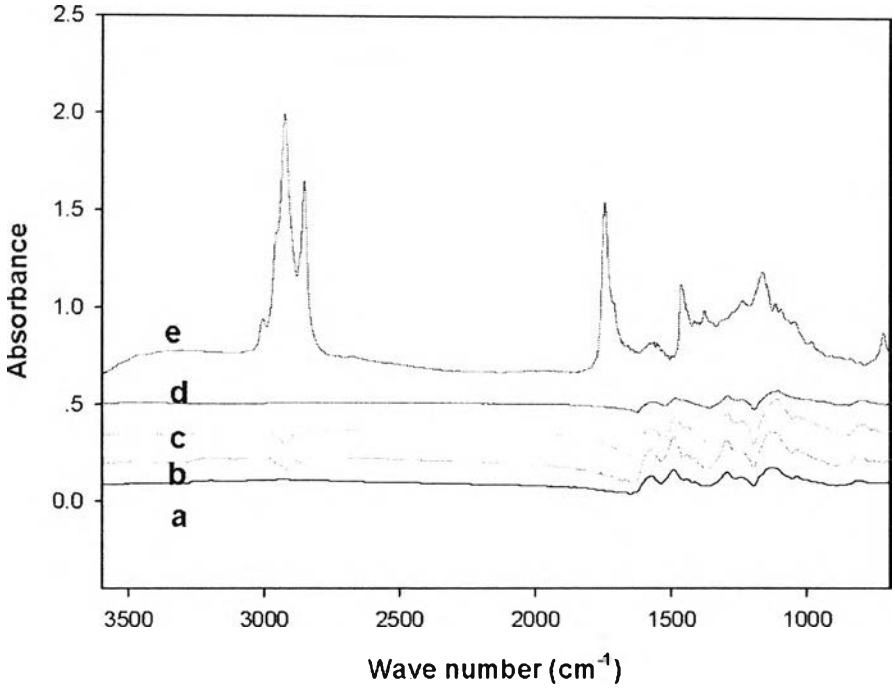

Figure 4.13 FTIR spectra of PANI synthesized at different ANI:Biosurfactant weight ratio using biosurfactant as a template, (a) 14.2:1; (b) 11.4:1; (c) 9.6:1 (d) conventional PANI; (e) Rhamnolipid biosurfactant.

4.4.2 UV-Vis Spectroscopy

The nanoparticles are highly water suspendable and the green-colored colloid solutions which are stable more than 12 hours at ambient conditions. In order to investigate the electronic states of PANI synthesized using biosurfactant as a template. The UV-vis spectra were used to confirm the electronic state of the synthesized PANI products. The PANI in emeraldine salt form (PANI ES), the conducting state of PANI, showed adsorption band at 410 nm, and a board band at 810 nm as shown in Figure 4.14. These indicated the conductive emeraldine salt structure: the first band corresponds to the cation radicals (polarons) and the second band related to the formation of bipolarons, respectively. The two bands relate to the doping level and formation of polaron band, which represent the protonation stage of the PANI chains. Additionally, the UV-vis spectra of PANI ES nanofibers synthesized by using biosurfactant as template are identical to that of PANI

synthesized by the conventional method. Therefore, it could be concluded that the addition of the biosurfactant template and the difference in ANI:Biosurfactant weight ratio did not alter the electronic state of the synthesized PANI product. Moreover, the UV-vis spectra of PANI salt form dissolved in N-Methyl-2-Pyrrolidone (NMP) solution was investigated as shown in Figure 4.14a. The UV-Vis spectra showed two absorption peaks at 330 nm and 630 nm. The two peaks imply the interaction between polyaniline and NMP. Since NMP is a highly polar solvent, the solvent-solvent interaction would be strong enough so the C=O group in the NMP molecule would like to deprotonate proton in the N-H segment of the polymer chain. This in turn would bring de-protonation of the polymer chain which would result in conversion of the salt phase into the insulating emeraldine base (PANI EB) (Rahy et al, 2008).

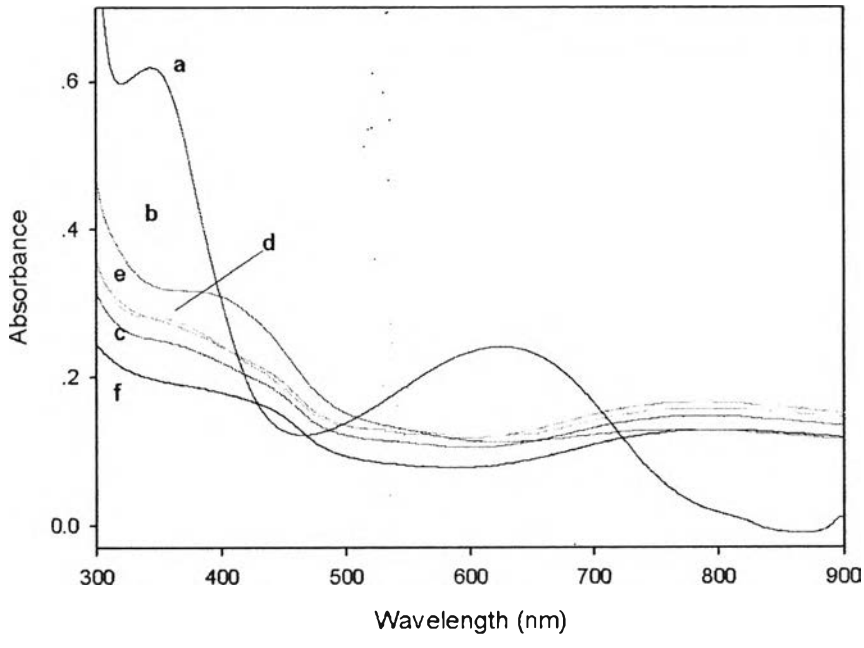

Figure 4.14 UV-vis spectra of synthesized polyaniline as a function of weigh ratio ANI:Biosurfactant a) PANI EB b) 11.3:1 c) 19.3:1 d) 22.7:1 e) 28.3:1 f) conventional PANI.

4.4.3 Thermal Analysis

Thermal property of biosurfactant, aniline monomer as well as PANI synthersized using various acid concentration were investigated as shown in Figure 4.15. The TGA thermogram of biosurfactant as shown in Figure 4.15-a demonstrated weight loss temperature at approximately 400 °C which correspond to decomposition temperature of biosurfactant. In contrast, the TGA thermogram of the resulting product (synthesized by using 0.1M, 0.5M and 1.0M HCl acid) after removal of biosurfactant template are showed 3 discrete weight loss at approximately 80, 280, 500°C as shown in Figure 4.15b. These are due to loss of water, elimination of dopant and degradation of polymer chains, respectively. However, degradation temperature of the obtained PANI after remove biosurfactant template also depent on acid concentration that using in the polymerization reaction. The TGA thermogram of PANI synthesized by using 0.01M HCl showed 3 discrete weight losses (Figure 4.15-c) at approximately 210°C, 280 and 380 °C which correlated to degradation of oligomer, loss of dopant molecule, and the remaining biosurfactant template, respectively. From the expriment, weight loss temperature of the obtained product at approximately 210 °C consistent with the weight loss temperature of aniline monomer (Figure 4.15-d) which illustrate decomposition temperature at approximately 190 °C. Furthermore, degradation temperaturte of the resulting product decreased from 500 °C to 210 °C when 0.01M HCl was used in the polymerization reaction. This result might be due to the acid concentration does not strong enough to obtain adequade anilinium ion (protonated aniline) attack to the reactive site, therefore, only oligomer structure was obtained and degradation temperature of the resulting product also decrease.

Figure 4.16 illustrate TGA thermogram of conventional PANI and PANI synthesized using biosurfactant as a template at various ANI: Biosurfactant weight ratios. All samples of the synthesized PANI showed three main weight-loss stages occurring at approximately 80, 280, and 500 °C. These weight losses were due to the loss of water and other volatiles (first weight-loss stage), the loss of acid dopant (second weight-loss stage), and decomposition of PANI (third weight-loss stage), respectively. These results indicate that the addition of biosurfactant template does not affect to the thermal property of the obtained PANI. Moreover, the

characteristic weight loss temperature of biosurfactant did not observe in the thermogram pattern of the resuting PANI, therefore, these appear results confirm complete removal of biosurfactant template.

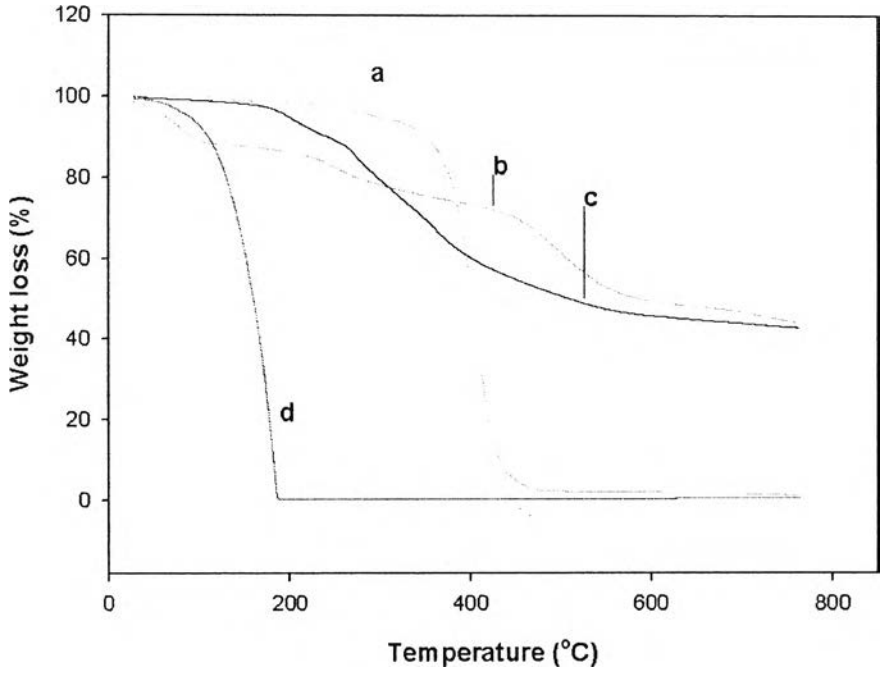

Figure 4.15 TGA thermograms of a) biosurfactant; PANI synthesized using various acid concentration b) 0.5M HCl, c) 0.01M HCl; d) aniline monomer.

Furthermore, the affects of reaction times at 4, 6, and 8 h on the thermal property were also investigated, as shown in Figure 4.17. It was found that all samples exhibits three discrete weight losses at approximately 80, 280, and 500 °C. Again the reaction time does not affect to the thermal stability of the obtained PANI.

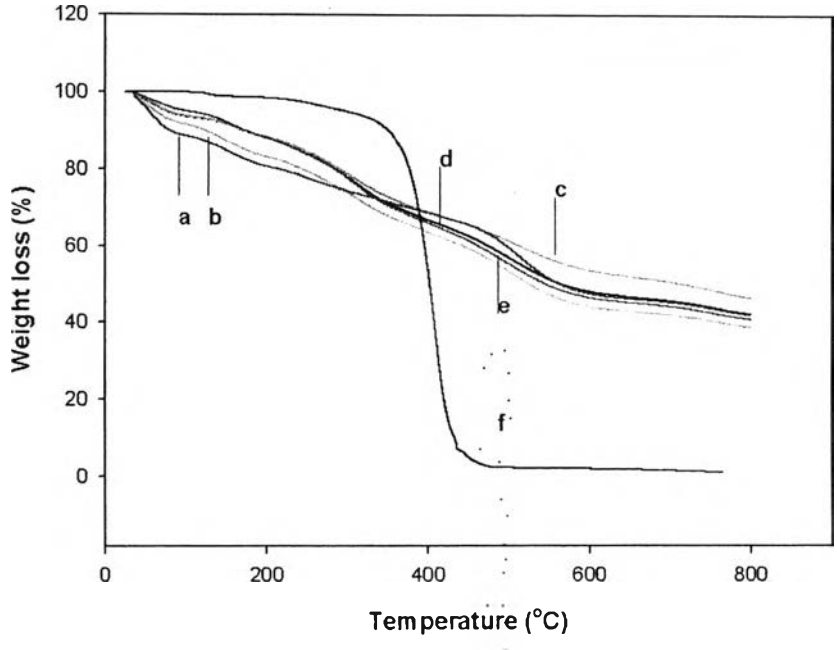

Figure 4.16 TGA thermograms of PANI synthesized using 1800 mg/L biosurfactant as a template at difference ANI:Biosurfactant weight ratio; a) 11.34, b) 19.28, c) 22.7, d)28.36, e) conventional PANI, and f) biosurfactant.

The affect of biosurfactant concentration on thermal property of the resulting PANI also was investigated as shown in Figure 4.18. The thermogram indicated that although increase the biosurfactant concentration from 1800 mg/L to 3600 mg/L, the thermogram still showed three main weight-losses stage at approximately 80, 280, and 500 °C. This result indicated that increasing of biosurfactant template in the reaction medium does not affect to thermal stability of the resulting PANI nanofibers.

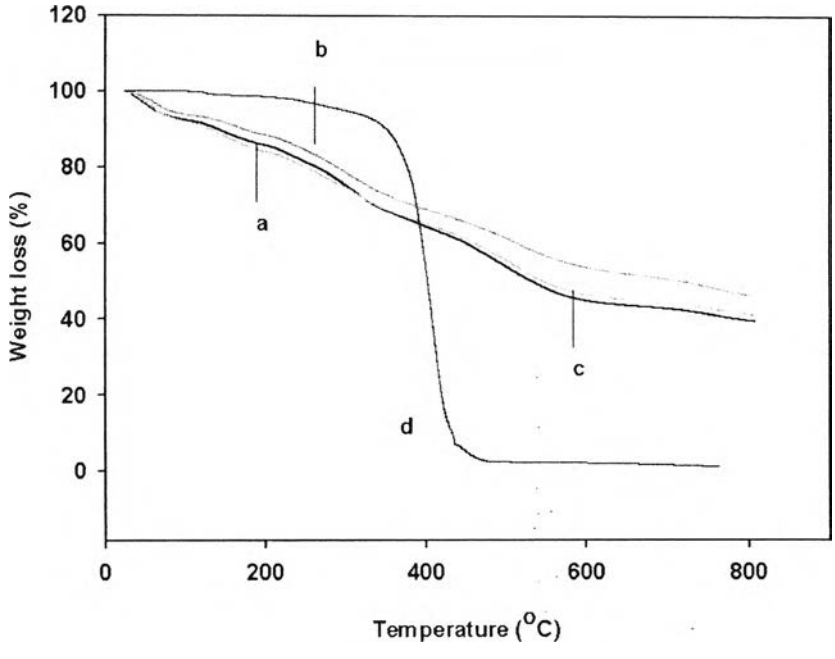

Figure 4.17 TGA thermograms of PANI synthesized at different polymerization time: a) 4 hr, b) 6 hr and c) 8 hr (ANI:Biosurfactant weight ratio of 22.7).

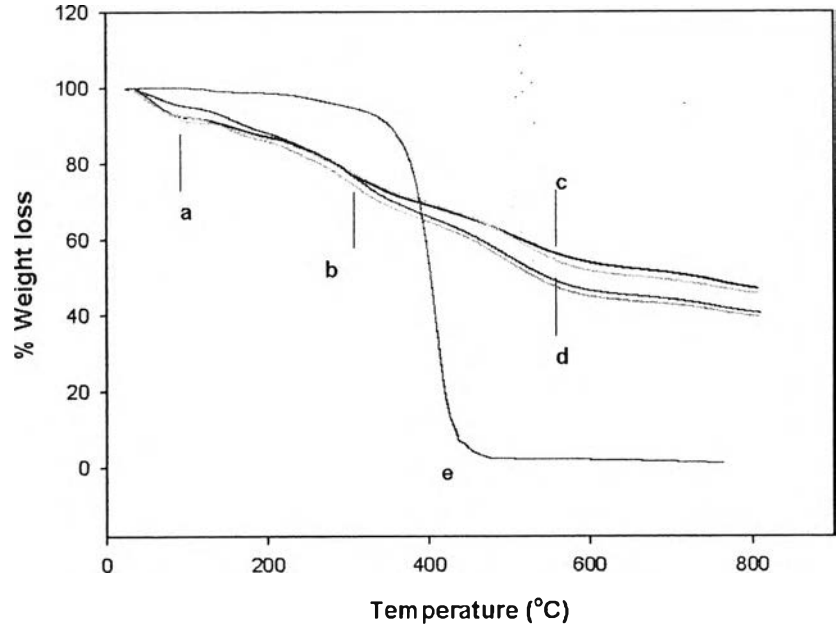

Figure 4.18 TGA thermograms of PANI synthesized using 3600 mg/L biosurfactant as a template at difference ANI:Biosurfactant weight ratio; a) 9.6, b) 11.4, c) 14.2, d) conventional PANI, and e) biosurfactant.

4.4.4 Wide Angle X-ray Diffraction (WAXD)

To further confirm the presence of the crystalline structure of the synthesized PANI, finely powdered HCl-doped PANI was subjected to wide angle X-ray diffraction analysis. The X-ray diffraction patterns of doped-PANI are given in Figure 4.19 and 2θ and *d*-spacing values are reported as well.

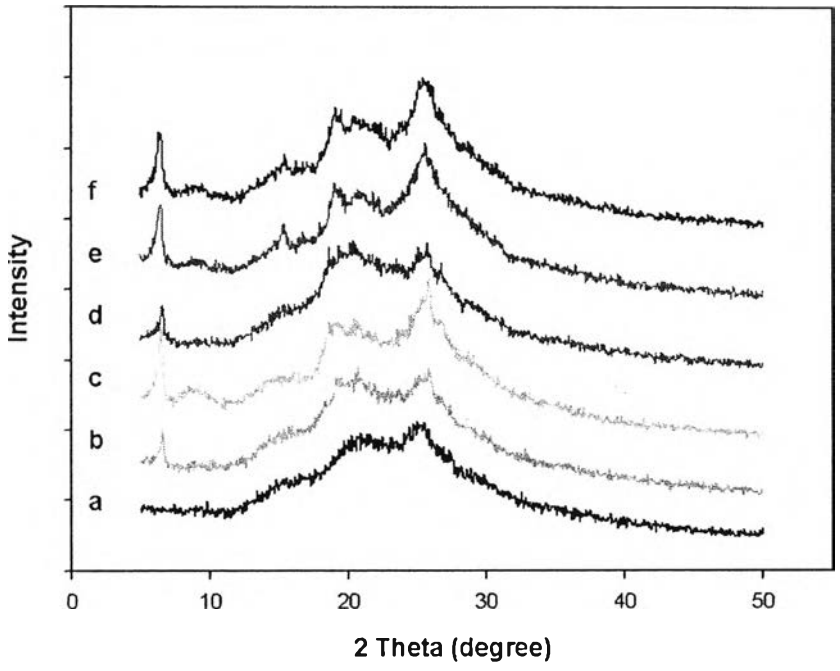

Figure 4.19 WXRD patterns of HCl-doped resulting PANI with the ANI:HCl composition ratio of 1:100 at different ANI:Biosurfactant weight ratio of (a) 11.3:1; (b) 19.3:1; (c) 22.7:1; (d) 28.3:1; and WXRD patterns of PANI synthesized by conventional approach at different ANI:HCl composition ratio of (e)1:100; (f) 1:25.

The XRD pattern of HCl-doped PANI synthesized at ANI:Biosurfactant weight ratio of 11.3:1 showed two broad peaks centered at 2θ = 20.0° and 25.6°(Figure 4.17-a), suggesting that the resulting PANI are amorphous. Zhang *et al.* (2002) revealed the X-ray scattering patterns of PANI doped with different kind of inorganic acid (HCl, H_2SO_4, HBF_4, and H_3PO_4). The patterns show two broad peaks centered at 2θ= 20° and 26° which indicated that the resulting PANI nanostructure are amorphous. On the other hand, The WXRD experiment of

HCl-doped PANI synthesized at ANI:Biosurfactant weight ratio of 19.3:1, 22.7:1, and 28.3:1 demonstrate three distinct peaks as shown in Figure 4.19b-d and table 4.4.

Table 4.3 WXRD data of HCl-doped PANI synthesized at different ANI:Biosurfactant weight ratio

ANI:Biosurfactant weight ratio	Peaks in WXRD	
	Peak at 2θ (deg)	*d*-spacing (Å)
a) 19.3:1	6.55, 19.25, 25.85	13.48, 4.60, 3.44
b) 22.7:1	6.60, 19.2, 25.85	13.38, 4.61, 3.44
c) 28.3:1	6.60, 20.05, 25.85	13.38, 4.42, 3.44

Han et al. (2008) and Zhang et al. (2002) reported that the peak centered at 2θ = 20° and 26° are ascribed to the periodicity parallel and perpendicular to the polymer chain, respectively. Chen et al. (2008) also reported that a special peak center at 6.9° arise from interplanar distance between polyaniline molecules or reflection to periodic distance between dopant and N atom on adjacent main chain. Moreover, Anikumar *et al.* (2007) indicated that the two peaks at 20.1 and 25.5° are generally observed in doped polyaniline, but the peak at 2θ = 6.4° is only observed for highly ordered samples in which the polyaniline chain distance increased by effective of dopant molecules. This result is consistent with the known partially-crystalline structure of PANI ES.

Anikumar *et al.* (2008) showed that the intensities ratio of the peaks at 2θ = 6.4° and 26° is directly related to crystallinity of polyaniline samples. The intensities ratio of the HCl-doped PANI at peaks 2θ = 6.55° and 25.85 are calculated as shown in table 4.4 and the crystallinity of HCl-doped conventional PANI using different ANI:HCl composition ratio also demonstrated in table 4.5.

Table 4.4 Crystallinity of HCl-doped PANI which using 1800 mg/l biosurfactant concentration at ANI:HCl composition ratio of 1:100

ANI:Biosurfactant weight ratio	intensity at 2θ=6.55	intensity at 2θ=25.85	crystallinity
a) 19.3:1	191	468	0.408
b) 22.7:1	431	684	0.630
c) 28.3:1	205	393	0.459

Table 4.5 Crystallinity of HCl-doped conventional PANI using various ANI:HCl composition ratio

ANI:HCl composition ratio	intensity at 2θ=6.55	intensity at 2θ=25.85	crystallinity
a)1:25	392	663	0.591
b)1:100	359	689	0.521

As appear results, it was found that the peak intensity ratio initially increase with increase the weight ratio and reach a maximum value for sample weight ratio of 22.7:1 and then decrease for higher weight ratio. From XRD studies it is indicated that in the case of the weight ratio equal to 22.7:1 the polymer chain are more ordered than any weight ratio after doped with 1.5M HCl acid. Additionally, the crystallinity of HCl-doped conventional PANI at different ANI:HCl composition ratio also were investigated. It was found that the degree of crystallinity of conventional PANI at composition ratio of 1:25 higher than ratio of 1:100. Anikumar et al. (2008) reported that the intensity ratio of the peak at 2θ = 6.4° and 25.9° were initially increased with increase the concentration of dopant and reach a maximum value for sample [aniline]/[dopant] equal to 450 and then gradually decreased for higher concentration of dopant. The X-ray diffraction data supports that the addition of biosurfactant as a template cause change in crystallinity of the HCl-doped PANI.

Moreover, the effect of polymerization time on the crystallinity of HCl-doped PANI also observed. The WXRD pattern of HCl-doped PANI at different polymerization times showed three distinct peaks as shown in Figure 4.20 and data also listed in table 4.6.

Table 4.6 WXRD data of HCl-doped PANI synthesized at different polymerization time (ANI:Biosurfactant weight ratio of 22.7:1)

ANI:Biosurfactant weight ratio	polymerization Time (h)	Peaks in WXRD	
		Peak at 2θ (deg)	*d*-spacing (Å)
a) 22.2:1	4	6.60, 20.90, 25.80	13.38, 4.24, 3.45
b) 22.7:1	6	6.60, 19.2, 25.85	13.38, 4.61, 3.44
c) 22.7:1	8	6.60, 20.90, 25.80	13.48, 4.24, 3.45

From the experiment, it was found that the highest in the intensities ratio ($I_{6.45}/I_{25.8}$) was observed at 6 hr polymerization time as shown in table 4.7. The highest degree of crystallinity this also indicated that the polymer chains of sample at this reaction time are more order than any reaction time. Additionally, the WXRD results consistent with the electrical conductivity measurement.

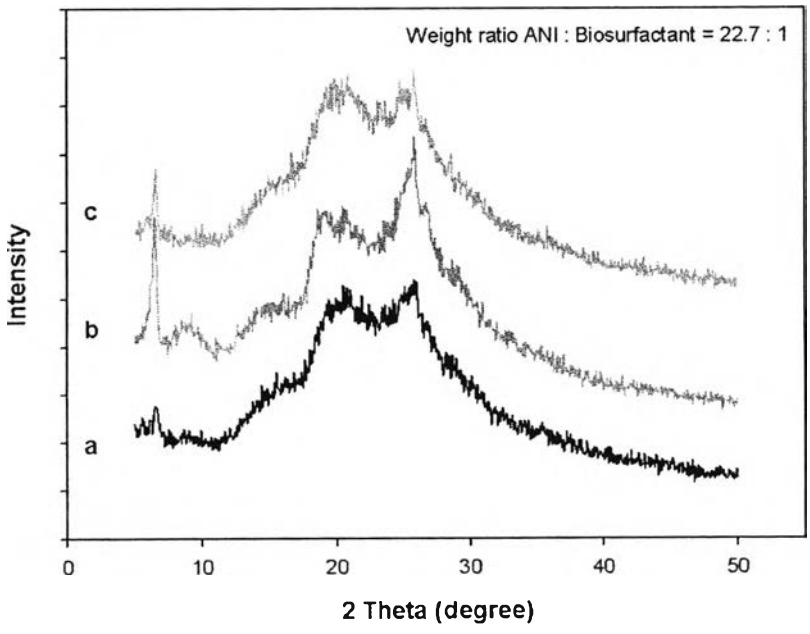

Figure 4.20 WXRD patterns of HCl-doped PANI at different polymerization time; (a) 4 hr; (b) 6 hr; (C) 8 hr (using the ANI:biosurfactant weight ratio of 22.7:1).

Table 4.7 Crystallinity of HCl-doped PANI which synthesized using 1800 mg/L biosurfactant concentration at different polymerization time

Polymerization time	intensity at 2θ=6.45	intensity at 2θ=25.85	crystallinity
4 hr	99	440	0.225
6 hr	431	684	0.630
8 hr	207	464	0.446

4.4.5 Electrical Property

4.4.5.1 Effect of Degree of Doping

In order to improve the electrical conductivity property, the degree of doping was studied. The electrical conductivities of the HCl-doped PANI pellets with the composition ratio of 1/5, 1/25, 1/50, 1/100, 1/200, and 1/300, where the composition are expressed in mole ratios of the repeat units of PANI to the hydrochloric acid units of polymeric acids, are investigated as shown in Figure 4.21. As appear result, instance of adding a biosurfactant as a template in the reaction medium, it was found that the electrical conductivities are initially increase from 0.1 ± 0.03 S/cm to 1.5 ± 0.2 S/cm to 3.7 ± 1.47 S/cm and 24.8 ± 1.69 S/cm when the composition ratio was increased from 1/5 to 1/25 to 1/50, and 1/100, respectively. and then gradually decrease for higher composition ratio (1/200 and 1/300). It was found that a maximum conductivity value of 24.8 S/cm was obtained at the composition ratio of 1/100.

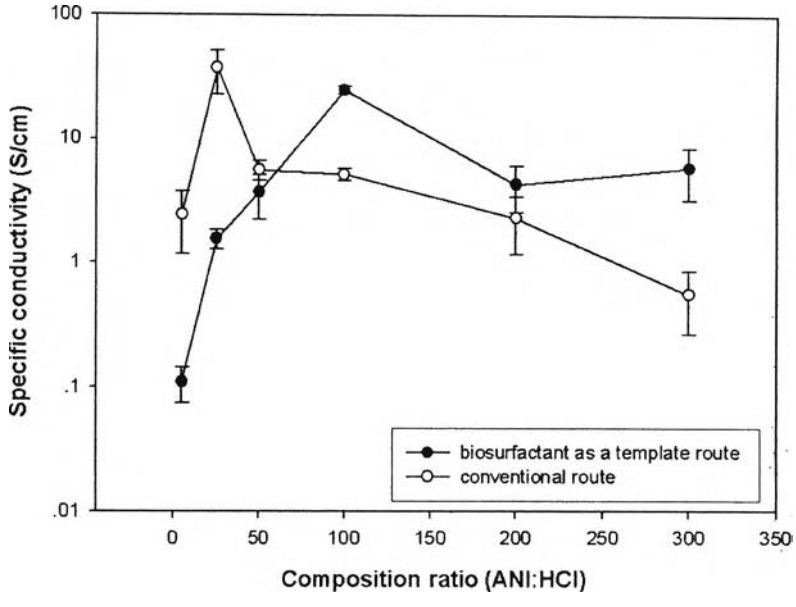

Figure 4.21 Room temperature conductivities versus the mole ratios of aniline units in PANI to the mole ratios of hydrochloric acid unit.

The enhancement of the electrical conductivity with increasing the composition ratio was due to the increasing degree of protonation of the imine group of PANI. In contrast, at higher the composition ratio (1/200 and 1/300), decreasing in electrical conductivity occurred. This result was probably due to occurred the over protonation of PANI chains causing a decrease in the delocalization length of PANI. From the degree of doping experiment, the electrical conductivities of the synthesized PANI at various ANI:Biosurfactant weight ratio were further investigated. However, the degree of doping of conventional route also was studied as shown in Figure 4.21. Initially, the electrical conductivity increase as function of the composition ratio and appear the maximum electrical conductivity value of 37.3 S/cm at a composition ratio of 1:25, and then gradually decreased as increasing the composition ratio this result due to over protonation take placed.

4.4.5.2 Effect of ANI:Biosurfactant Weight Ratio

The experiment indicated that the electrical conductivity of the dedope PANI decreased with increasing the ANI:Biosurfactant weight ratio as shown in Figure 4.22 and also listed in Table 4.8. On the other hand, after dope with

1.5 M HCl acid at the composition ratio of 1/100 shown in Figure 4.17 and data are also listed in Table 4.8. It was found that the electrical conductivity initially increase with increase in the weight ratio and reach the maximum electrical conductivity value of 24.8 S/cm at the weight ratio of 22.7:1 after that the electrical conductivity was decreased as increase the weight ratio to 28.3:1. Yang et al. (2005) reported that the maximum electrical conductivity was obtained at mole ratio of ANI/aminobenzenesulfonic acid (SAN), SAN acted as a self-doping monomer and a surfactant, equal to 1.0 after that the electrical conductivity decreased with increasing the ANI/SAN ratio at ANI/SAN > 1 due to decrease in doping degree predominant. However, the electrical conductivity also depends on alignment of polymer chain. Sambhu et al. (2009) revealed that higher conductivity will most likely be due to its high crystallinity. These appear result consistence with the XRD results as shown in table 4.4 which can observe that the highest degree of crystallinity was obtained at the weight ratio of 22.7:1 and then crystallinity decreased as increase weight ratio to 28.3:1.

Table 4.8 Electrical conductivities of pelletized HCl-doped PANI samples at composition ratio of 1:100

ANI:Biosurfactant weight ratio	Specific conductivity (S/cm)	
	Undoped state	Doped state
a)11.3:1	6.09E-04±1.16E-05	0.139±0.019
b)19.3:1	5.60E-04±5.77E-05	0.143±0.021
c)22.7:1	5.19E-04±2.57E-05	24.834±1.698
d)28.3:1	1.15E-04±8.45E-06	6.580±3.087

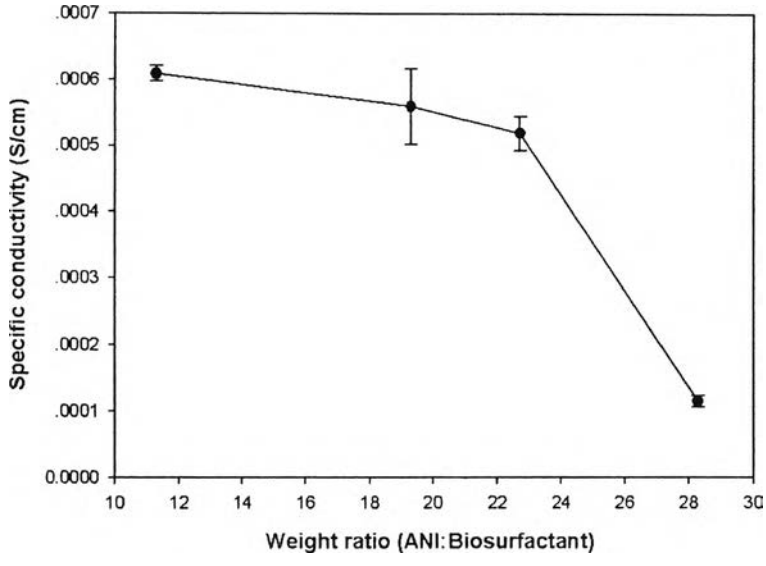

Figure 4.22 Specific conductivity of dedope PANI as a function of ANI:Biosurfactant weight ratio.

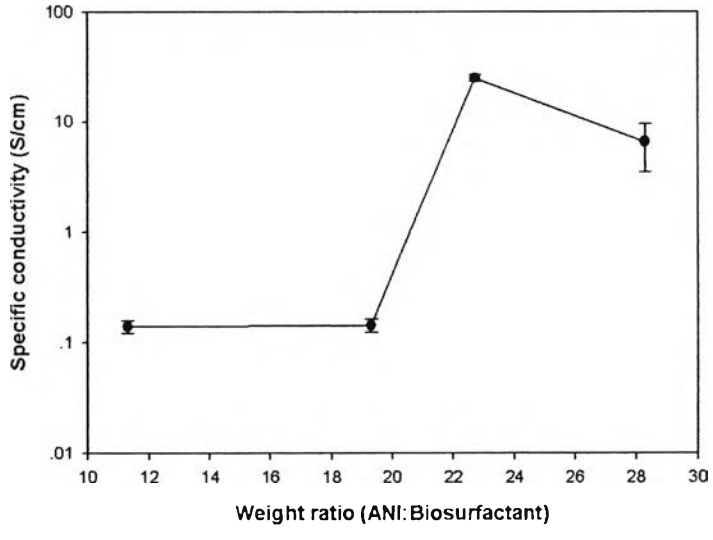

Figure 4.23 Specific conductivity of HCl-doped PANI as a function of ANI:Biosurfactant weight ratio.

4.4.5.3 Effect of Polymerization Time

The effect of polymerization time on the electrical conductivity was also investigated as shown in table 4.9. The maximum electrical

conductivity of 24.8 S/cm was obtained at the polymerization time of 6 hr and then as increase the polymerization time to 8 hours, the electrical conductivity was decreased to 3.9 S/cm. The results agreed with those of previous works (Saravanan et al, 2007) which reported that when further increasing the polymerization time from 8 to 12 h, conductivity decreases from 0.06 to 0.02 S/cm. These appear results need to concern about the alignment of polymer chains . However this results consistent with the XRD experiment as shown in table 4.5. The data also showed that PANI synthesized at 6 hr polymerization time causing polymer chains are more order than PANI synthesized at any polymerization time.

Table 4.9 Electrical conductivities as function of polymerization times of pelletized HCl-doped PANI samples

ANI:Biosurfactant weight ratio	Polymerization Time (hr)	Specific conductivity (S/cm)	
		Undoped state	Doped state
22.7:1	4	2.47E-04±4.82E-06	0.785±0.076
22.7:1	6	5.19E-04±2.59E-05	24.834±1.698
22.7:1	8	2.94E-04±4.15E-05	3.923±2.342